

Omnidirectional Video

Christopher Geyer and Kostas Daniilidis*
GRASP Laboratory, University of Pennsylvania, Philadelphia, PA 19104
{cgeyer, kostas}@seas.upenn.edu

Keywords: catadioptric cameras, structure from motion, pose estimation, immersive walk-throughs.

Abstract

Omnidirectional video enables direct surround immersive viewing of a scene by warping the original image into the correct perspective given a viewing direction. However, novel views from viewpoints off the camera path can only be obtained if we solve the 3D motion and calibration problem. In this paper we address the case of a parabolic catadioptric camera – a paraboloidal mirror in front of an orthographic lens – and we introduce a new representation, called the circle space, for points and lines in such images. In this circle space, we formulate an epipolar constraint involving a 4x4 fundamental matrix. We prove that the intrinsic parameters can be inferred in closed form from the 2D subspace of the new fundamental matrix from two views if they are constant or from three views if they vary. Three dimensional motion and structure can then be estimated from the decomposition of the fundamental matrix.

*The authors are grateful for support through the following grants: NSF-IIS-0083209, NSF-EIA-0218691, NSF-IIS-0121293, NSF-EIA-9703220, and a GAANN fellowship.

List of Figures

1	Projection of a scene point P to an image point P' through reflection on the mirror and projection from a point at infinity.	5
2	A circle γ is represented by the point $\tilde{\gamma}$. The plane π is the polar plane of $\tilde{\gamma}$ with respect to Π . γ is obtained by projecting the intersection of π with Π to the plane. . .	7
3	The images of the absolute conic $\tilde{\omega}$ and calibrating conic $\tilde{\omega}'$ lie the same vertical distance, $4f^2$, away from paraboloid Π . The calibrating conic $\tilde{\omega}'$ which is the projection of the frontoparallel horizon lies in a plane containing the circle space representations of all projections of lines in the world (all of them intersect antipodally to the image center). This plane is the polar plane to the absolute conic $\tilde{\omega}$ with respect to paraboloid Π	9
4	The paraboloid with points in space and their projection before (left) and after (calibration). The image of the absolute conic is mapped to the focus and the paraboloid remains invariant but not pointwise. Points on the paraboloid move to the right positions so that the rays through the unique viewpoint go through the original scene points.	10
5	Two images taken with the same parabolic catadioptric camera. Points are those used for correspondence. Points highlighted in white are on the ground plane; points highlighted in black are on one side of the building facade.	14
6	Reconstruction from two images. Black points are in the ground plane. Darkly shaded points are on the front facade of the building; lightly shaded points are on the other facade (which is on the left in the images). Planes are fitted to the facade and ground plane (and translated slightly so points are made visible). The coordinate systems at the points are the pose estimates. Tilt of the fitted plane is irrelevant to the results of the reconstruction. The top view is taken looking straight at the front facade; the bottom view is from the side. Note that the mirror reverses the orientation; this has been accounted for in the reconstruction.	15

1 Introduction

Surround sensing is one of the main factors increasing the subjective feeling of presence in a remote environment. It was very early recognized, that recording an omnidirectional video (Rees, 1971) could be replayed on a head-mounted display (Boult, 1998) which would show the correct viewing direction upon sensed head turning. In parallel, the wide dissemination of images over the web enabled also the popularization of panoramic photography with tools like QuicktimeVR (Chen & Williams, 1993). It is almost standard nowadays, to watch an unvisited real-estate, hotel, or a historical landmark, through a virtual panning interface. The popularity of panoramic visualization boosted a series of new panoramic sensors. Because mechanical devices rotating a camera about an axis through its optical center can not allow capturing dynamic events, designers turned to mirrors or clusters of outwards looking cameras. The reader is referred to the site of omnidirectional vision <http://www.cis.upenn.edu/~kostas/omni.html> where the links to more than a dozen designs reside. Though clusters of cameras might have higher resolution in terms of pixels per sterangle they can never produce a parallax free panorama because the optical centers are only approximately coincident. The solution to the uniqueness of an effective viewpoint has been provided by combinations of lenses (dioptric) and mirror (catoptric) surfaces of revolution with quadratic profile. Such sensors are called catadioptric and the ones providing a single viewpoint are called **central catadioptric**. Several authors have studied the properties of central catadioptric cameras and the image formation in them (Nayar, 1997; Svoboda, Pajdla, & Hlavac, 1998; Bruckstein & Richardson, 2000; Yagi, Kawato, & Tsuji, 1994; Kang, 2000; Geyer & Daniilidis, 2001a). Kang (2000) proposed a single view approach from the image of the circular mirror boundary of a paraboloid mirror. Geyer and Daniilidis (2002a, 2001a) showed how calibration of a parabolic catadioptric system can be achieved from a single view of three lines in space or from a single view of two sets of parallel lines. For an extensive coverage of catadioptric sensor design the reader is referred to the recent book by Benosman and Kang (2000) and the proceedings of the Workshops for Omnidirectional Vision (Daniilidis, 2000; Benosman & Mouaddib, 2002).

The feeling of immersion is increased not only by the possibility to turn your head and obtain the correct viewing direction but also by changing viewpoint. This is the basis of image based rendering where in the extreme case of a lightfield (Levoy & Hanrahan, 1996) or a lumigraph (Gortler, Grzeszczuk, Szeliski, & Cohen, 1996) the scene is captured from almost every viewing position and direction. In case of an omnidirectional video, Taylor (2000) and Aliaga (2001) estimated the camera pose based on special features like vertical edges so that a walkthrough over the same path taken by the camera can be made. However, no new views have been synthesized.

The question of synthesizing novel views in case of an unknown environment is equivalent to solving the problem of structure from motion given an uncalibrated sequence of images. Then if the camera parameters and the euclidean motion of the camera is estimated, a view from a new given position can be synthesized if we establish dense correspondences between the views of the video closest to the new position. We will not deal with the problem of correspondence in this paper. We have provided real-time solutions for trilinear perspective (Mulligan, Isler, & Daniilidis, 2002) and first results in the challenging case of omnidirectional imagery (Daniilidis, Makadia, & Bülow, 2002). The question of estimating the 3D-motion and intrinsic parameters of a camera from point correspondences in conventional perspective video is a thoroughly studied problem. We are not going to review here the vast amount of literature on uncalibrated Euclidean reconstruction which has been comprehensively summarized in the two recent books (Hartley & Zisserman, 2000; Faugeras, Luong, & Papadopoulos, 2001). The main result (Maybank & Faugeras, 1992) is that three views suffice for Euclidean reconstruction with all intrinsics unknown but constant. The results

still hold for known aspect ratio and skew. Hartley (2000) showed that a varying focal length can be recovered from two views with all other intrinsic parameters fixed. Sturm (1999) studied the degenerate configurations for the same assumption. Heyden and Astrom (1997) proved that four views suffice for unknown varying focal length and image center but known aspect ratio and skew. Pollefeys et al. (1998) studied several configurations of unknown and varying parameters.

A main concern in all the above structure from motion algorithms is their sensitivity to noise. It has been proved in the past (Daniilidis & Spetsakis, 1996; Jepson & Heeger, 1990; Maybank, 1993) that the smaller is the field of view the higher is the error effect of the coupling between rotation and translation estimates. The shape of the imaging surface combined with the field of view affect also sensitivity and indeed Fermueller and Aloimonos (1998) proved the superiority of the sphere over the plane regarding stability.

In the omnidirectional vision literature, there are very few approaches dealing with structure from motion. Gluckman and Nayar (1998) studied ego-motion estimation by mapping the catadioptric image to the sphere. Svoboda et al (1998) first established the epipolar geometry for all central catadioptric systems. Kang (2000) proposed a direct self-calibration by minimizing the epipolar constraint. Teller (2000) showed how to compute ego-motion from spherical mosaics. Sturm (2002) used the model presented here and in (Geyer & Daniilidis, 2001b) to compute the motion between catadioptric and perspective views. Barretto and Araujo (2002) used the model in (Geyer & Daniilidis, 2001a) for self-calibration.

The question we are going to study in this paper is, given an uncalibrated catadioptric video using a mirror of parabolical profile and an orthographic lens, how can we estimate the 3D motion of the camera and the focal length (combined scaling factor of mirror, lens, and CCD-chip) and the image center (intersection of the optical axis with the image plane).

The answer is that the solution is much simpler than in the perspective case – it involves only a singular value decomposition and needs fewer frames than in the perspective case. Its simplicity makes it useful not only for novel view synthesis but also as new localization (tracking) sensor for augmented reality, in particularly useful in outdoors environments where optical or magnetic trackers can hardly be used.

Let us briefly sketch the solution. It is already known that in parabolic catadioptric systems lines project onto circles. We introduce a new representation for circles in the image plane: the circle space of three dimensions. This space is divided into two parts by an abstract paraboloid. Such an abstraction is not new in the graphics community. A similar paraboloid has been used in the past to compute the Voronoi diagram of a point set from the intersection of the tangent planes at the lifted points. The exterior of our paraboloid represents all circles with real radius and the interior all circles with imaginary radius. The space does not contain circles with complex radii but the paraboloid itself represents all circles with zero radius which are just points on the plane. By lifting each image point to a point of the paraboloid and each image circle to a point outside the paraboloid we have one space for both points and circles.

The fact that we can represent imaginary circles enables us to represent the image of the absolute conic (Maybank, 1993) which encodes the entire intrinsic calibration information. In the calibrated case, the image of the absolute conic is the focus of the abstract paraboloid in the circle space. In the non-calibrated case, the imaginary image of the absolute conic is a point inside the abstract paraboloid that is vertically symmetric to the point representing the real image of the fronto-parallel horizon.

We formulate the calibration problem as the question for a linear transformation that will map uncalibrated points on the abstract paraboloid to “calibrated” points on a paraboloid and the image of the absolute conic to its focus. Indeed, such a linear transformation K exists and encodes

all three intrinsic parameters (focal length and image center). The question is now to find this mapping from multiple views.

It turns out that we can formulate the epipolar constraint using projective coordinates of the circle space we have been working on. A new 4×4 “catadioptric” fundamental matrix is composed from the essential matrix E and an induced projection following the mapping K above. We prove that the circle representation of the images of the absolute conic in the left and the right view respectively lie in the left and right nullspaces of the catadioptric fundamental matrix. Because the catadioptric fundamental matrix is rank 2, the image of the absolute conic is in the intersection of the left and right nullspace if the intrinsic parameters are constant and rotation does not vanish and is not about the translation direction. For three views, it is even possible to determine the image of the three different absolute conics in the case of varying intrinsics.

Thus, the main result of this paper is that, with unknown focal length and image center, Euclidean reconstruction from parabolic catadioptric views is feasible:

- From two views with the same camera parameters.
- From three views with varying camera parameters.

In both cases, it is one view less, than in the case of perspective views with the same unknowns (focal length and image center): Three views are necessary for constant parameters (Maybank & Faugeras, 1992; Ma, Soatto, Kosecka, & Sastry, 2000) and four views are necessary for varying parameters (Heyden & Aström, 1997).

In the next section we mention introductory facts about catadioptric geometry. We introduce the notion of circle space and we find the image of the absolute conic on that space. We finish the second section with the recovery of the image of the absolute conic from the catadioptric fundamental matrix. In the third section we present reconstruction algorithms for two and three views. In the fourth section a real experiment is described.

2 Catadioptric plane representations

We recall from (Geyer & Daniilidis, 2002a) some facts about the projection induced by a parabolic mirror.

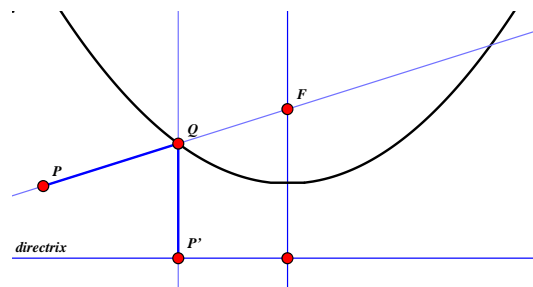


Figure 1: Projection of a scene point P to an image point P' through reflection on the mirror and projection from a point at infinity.

Fact 1. In a coordinate system whose origin is the focus of the paraboloid and axis of symmetry coincides with the z -axis, the projection of a space point $P = (x, y, z, 1)$ to a point P' in the image

reads (Fig. 1)

$$\begin{pmatrix} u \\ v \\ 1 \end{pmatrix} = \begin{pmatrix} c_x + \frac{2fx}{-z + \sqrt{x^2 + y^2 + z^2}} \\ c_y + \frac{2fy}{-z + \sqrt{x^2 + y^2 + z^2}} \\ 1 \end{pmatrix}, \quad (1)$$

where f is the combined focal length of the mirror and camera, and (c_x, c_y) is the image center, the intersection of the axis of the parabola with the image plane. We assume that the aspect ratio is 1 and that there is no skew. The image point is obtained by intersecting the ray through the focus and the space point with the parabola, then orthographically projecting the intersection to a plane perpendicular to the axis of the paraboloid.

Fact 2. The horizon of the fronto-parallel plane, the plane perpendicular to the axis of the paraboloidal mirror, is the circle

$$(c_x - u)^2 + (c_y - v)^2 = 4f^2. \quad (2)$$

This circle of radius $2f$ centered about the image center is the equivalent of the calibrating conic which we call ω' since we call the image of the absolute conic ω .

Fact 3. The projection of a line is an arc of a circle. If ξ is the center and R the radius of the circle and if $d^2 = (c_x - \xi_x)^2 + (c_y - \xi_y)^2$ then

$$4f^2 + d^2 = R^2. \quad (3)$$

This condition is equivalent to the condition that the circle intersect ω' antipodally.

Fact 4. The image ω of the absolute conic Ω_∞ is the circle

$$(c_x - u)^2 + (c_y - v)^2 = -4f^2, \quad (4)$$

centered at the image center with radius $2if$. This can be derived by solving for x and y in the projection formula (1) after substituting $x^2 + y^2 + z^2 = 0$,

$$x = \frac{(u - c_x)z}{2f} \quad y = \frac{(v - c_y)z}{2f}.$$

substitute the right hand sides into $x^2 + y^2 + z^2 = 0$, obtaining

$$\frac{z^2}{4f^2} (4f^2 + (c_x - u)^2 + (c_y - v)^2) = 0.$$

Dividing by $z^2/4f^2$ leaves (4). Thus, knowledge of either the absolute conic or the calibrating conic yields the intrinsic parameters.

2.1 Parabolic Circle Space

In the next few paragraphs we consider an abstract paraboloid which is different from the physical paraboloid of the mirror. Following (Pedoe, 1970), we use this surface to describe a correspondence between points in space and circles in the plane. Lines in this circle space correspond to one parameter systems of coaxial circles. Planes in the space correspond to two parameter systems of circles which intersect a single circle antipodally. See Figure 2 in which a circle is obtained from a

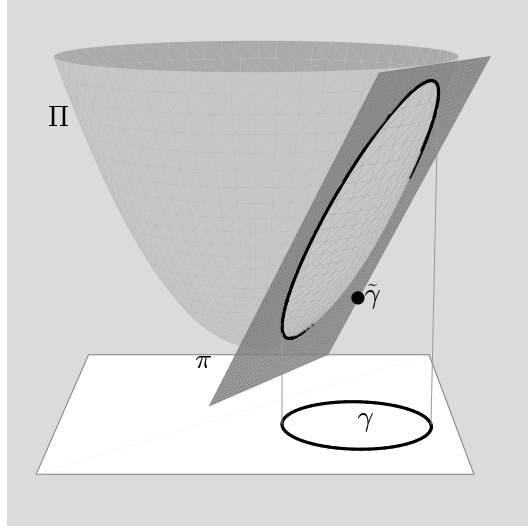


Figure 2: A circle γ is represented by the point $\tilde{\gamma}$. The plane π is the polar plane of $\tilde{\gamma}$ with respect to Π . γ is obtained by projecting the intersection of π with Π to the plane.

point in space by taking the polar of the point with respect to the paraboloid, and projecting to a plane the intersection of the polar plane with the paraboloid; this projection will be a circle.

We call the paraboloid Π ; it is given by the quadratic form

$$C_{\Pi} = \begin{pmatrix} 1 & 0 & 0 & 0 \\ 0 & 1 & 0 & 0 \\ 0 & 0 & 0 & -\frac{1}{2} \\ 0 & 0 & -\frac{1}{2} & -\frac{1}{4} \end{pmatrix}. \quad (5)$$

Its focus is at the origin and has a focal length equal to $\frac{1}{4}$. So,

$$\Pi = \{p : p^T C_{\Pi} p = 0\} = \left\{ (x, y, x^2 + y^2 - 1/4, 1)^T \right\}.$$

Definition. Suppose γ is the circle centered at (p, q) with radius R :

$$(p - x)^2 + (q - y)^2 = R^2, \quad (6)$$

where R is possibly zero or imaginary, but never complex. Let the point representation of γ be the the projective point

$$\tilde{\gamma} = \left(p, q, p^2 + q^2 - R^2 - \frac{1}{4}, 1 \right)^T. \quad (7)$$

Note that the circle's radius is real iff it lies outside of Π . Its radius is imaginary iff it lies inside of (above) Π . If $R = 0$ then γ is a single point and $\tilde{\gamma}$ lies on Π . The set of points $\{\tilde{\gamma}\}$ is the parabolic circle space.

When γ is a point, because $\tilde{\gamma}$ has the same x and y coordinates as γ but lying on Π , we say that $\tilde{\gamma}$ is the lifting of γ to Π .

Proposition. *If π is the polar plane of the point $\tilde{\gamma}$ with respect to the paraboloid Π , the orthographic projection in the direction of the z -axis of the intersection of π with Π is the circle γ .*

Proof: The implicit equation of the polar plane π of $\tilde{\gamma}$ is

$$\begin{aligned} 0 &= \tilde{\gamma}^T C_{\Pi} (x \ y \ z \ 1)^T \\ &= \frac{1}{2} \left(-\frac{1}{4} - p^2 - q^2 + 2px + 2qy - z \right). \end{aligned}$$

substitute $z = x^2 + y^2 - 1/4$, yielding (6). □

Therefore the point $(p, q, r, 1)$ represents the circle

$$(p - x)^2 + (q - y)^2 = p^2 + q^2 - r - \frac{1}{4}. \quad (8)$$

We can extend the definition to encompass lines as well; they are represented by points on the plane at ∞ . The polar plane of a point $(p, q, r, 0)$ at infinity is the plane

$$0 = -\frac{r}{2} + px + qy,$$

which is independent of z and so the line in the plane has the same equation.

2.2 Application of Circle Representation

First, note the point representations of the calibrating conic,

$$\tilde{\omega}' = \left(c_x, c_y, c_x^2 + c_y^2 - 4f^2 - \frac{1}{4}, 1 \right)^T, \quad (9)$$

which, because it has a real radius, lies outside of Π ; and the absolute conic,

$$\tilde{\omega} = \left(c_x, c_y, c_x^2 + c_y^2 + 4f^2 - \frac{1}{4}, 1 \right)^T, \quad (10)$$

which, because it has an imaginary radius, lies inside of Π . The points $\tilde{\omega}$ and $\tilde{\omega}'$ lie the same vertical distance, $4f^2$, away from Π (Fig. 3).

Proposition. *The point representations of circles which are images of lines in a parabolic projection lie in a plane whose pole with respect to Π is $\tilde{\omega}$.*

Proof: If $(p, q, r, 1)$ is a circle which is the parabolic projection of a line it must satisfy (3). Using (8),

$$\begin{aligned} 4f^2 + (c_x - p)^2 + (c_y - q)^2 &= p^2 + q^2 - r - \frac{1}{4} \\ 4f^2 + c_x^2 + c_y^2 + \frac{1}{4} &= 2pc_x + 2qc_y - r, \end{aligned} \quad (11)$$

which, in the variables p, q , and r , is the equation of a plane. This plane is represented by the row vector

$$\pi = (c_x, c_y, -1/2, -2f^2 - c_x^2/2 - c_y^2/2 - 1/8).$$

The point

$$C_{\Pi}^{-1} \pi^T = (c_x, c_y, c_x^2 + c_y^2 + 4f^2 - 1/4, 1) = \tilde{\omega},$$

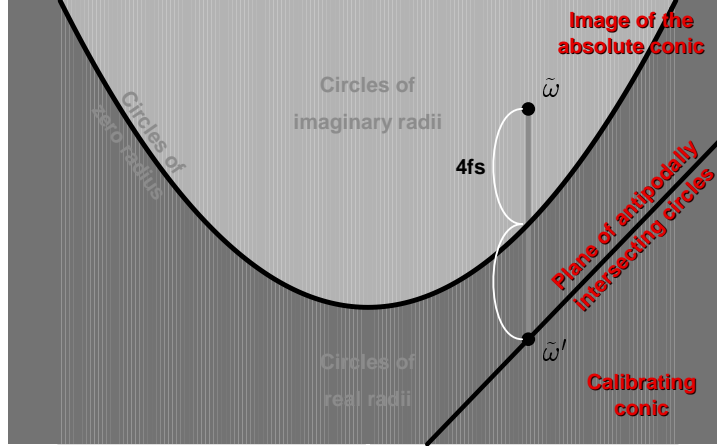


Figure 3: The images of the absolute conic $\tilde{\omega}$ and calibrating conic $\tilde{\omega}'$ lie the same vertical distance, $4f^2$, away from paraboloid Π . The calibrating conic $\tilde{\omega}'$ which is the projection of the frontoparallel horizon lies in a plane containing the circle space representations of all projections of lines in the world (all of them intersect antipodally to the image center). This plane is the polar plane to the absolute conic $\tilde{\omega}$ with respect to paraboloid Π .

is the pole of the plane π . □

The paraboloid Π was defined so that its focus is the origin. The point $\tilde{\omega}$ is located at the origin when $c_x, c_y = 0$ and $f = \frac{1}{4}$. The polar plane of this point (11) reduces to $r = -\frac{1}{2}$. In this case, image points lifted to the parabola exactly correspond to calibrated rays. When these intrinsics hold, the lifting of a space point projected by formula (1) is a point on the parabola which is collinear with the focus and the point in space. In particular, the projection of the point $(x, y, z, 1)^T$ in space is

$$\left(\frac{\frac{1}{2}x}{-z + \sqrt{x^2 + y^2 + z^2}}, \frac{\frac{1}{2}y}{-z + \sqrt{x^2 + y^2 + z^2}}, 1 \right)^T,$$

according to (1). The lifting of this point is,

$$\begin{pmatrix} \frac{\frac{1}{2}x}{-z + \sqrt{x^2 + y^2 + z^2}} \\ \frac{\frac{1}{2}y}{-z + \sqrt{x^2 + y^2 + z^2}} \\ \frac{\frac{1}{4}x^2 + \frac{1}{4}y^2}{(-z + \sqrt{x^2 + y^2 + z^2})^2} - \frac{1}{4} \\ 1 \end{pmatrix} \propto \begin{pmatrix} x \\ y \\ z \\ -2z + 2\sqrt{x^2 + y^2 + z^2} \end{pmatrix}$$

which lies on the line through the focus and the point $(x, y, z, 1)^T$.

Is there a linear transformation which transforms point representations of uncalibrated image points, in which $\tilde{\omega}$ is in general position, to calibrated rays, in which $\tilde{\omega}$ is the origin? In the next section we show that this is indeed the case.

2.3 Transformations Fixing Π

In this section we find linear transformations under which Π is invariant. In particularly we are interested in transformations which map the image of the absolute conic to the center of the

paraboloid as illustrated in Fig. 4.

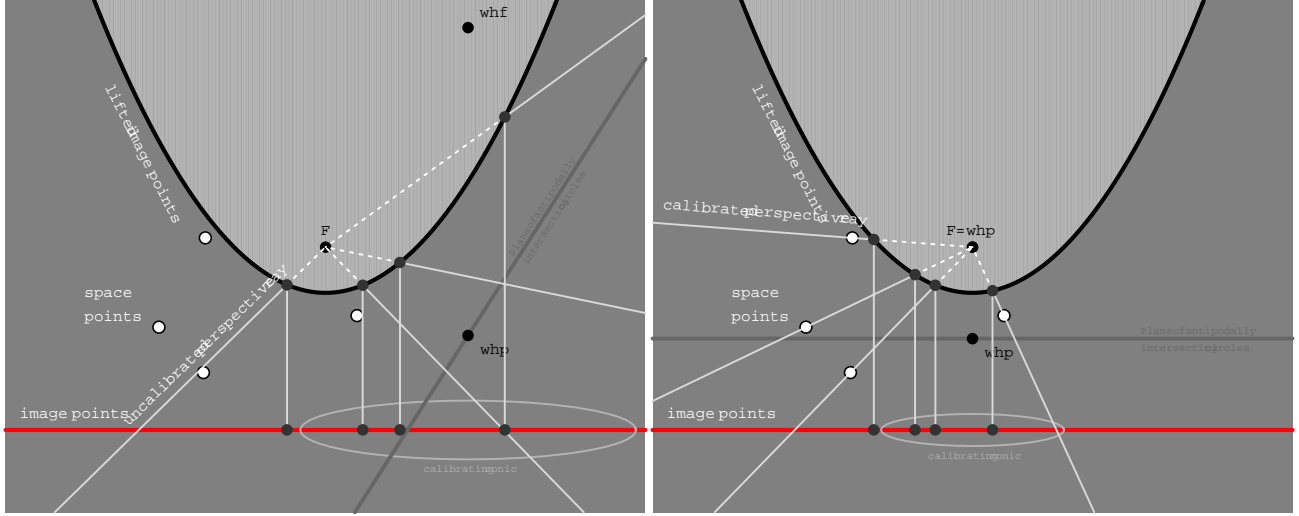


Figure 4: The paraboloid with points in space and their projection before (left) and after (calibration). The image of the absolute conic is mapped to the focus and the paraboloid remains invariant but not pointwise. Points on the paraboloid move to the right positions so that the rays through the unique viewpoint go through the original scene points.

The four transformations,

$$R_\theta = \begin{pmatrix} \cos \theta & \sin \theta & 0 & 0 \\ -\sin \theta & \cos \theta & 0 & 0 \\ 0 & 0 & 1 & 0 \\ 0 & 0 & 0 & 1 \end{pmatrix}, \quad S_\alpha = \begin{pmatrix} \alpha & 0 & 0 & 0 \\ 0 & \alpha & 0 & 0 \\ 0 & 0 & \alpha^2 & \frac{\alpha^2-1}{4} \\ 0 & 0 & 0 & 1 \end{pmatrix},$$

$$T_\tau = \begin{pmatrix} 1 & 0 & 0 & \tau_x \\ 0 & 1 & 0 & \tau_y \\ 2\tau_x & 2\tau_y & 1 & \tau_x^2 + \tau_y^2 \\ 0 & 0 & 0 & 1 \end{pmatrix}, \quad H = \begin{pmatrix} -1 & 0 & 0 & 0 \\ 0 & 1 & 0 & 0 \\ 0 & 0 & 1 & 0 \\ 0 & 0 & 0 & 1 \end{pmatrix},$$

are such that for any choice of θ , α , and vectors τ ,

$$R_\theta^T C_\Pi R_\theta \propto C_\Pi, \quad S_\alpha^T C_\Pi S_\alpha \propto C_\Pi, \\ T_\tau^T C_\Pi T_\tau \propto C_\Pi, \quad H^T C_\Pi H \propto C_\Pi,$$

where C_Π was previously defined in (5) and is the quadratic form of Π . Therefore these transformations affect the parabolic circle space such that they take points to points, as opposed to say points to circles. The transformations have the following effect on points in the image plane: R_θ induces a rotation of θ about the origin; S_α induces a scale of α also about the origin; T_τ translates points by τ ; and H reflects about the line $x = 0$.

Any composition of these transformations will also leave Π invariant. Note that these transformations also leave π_∞ invariant. They are therefore affine transformations, and also they send lines to lines.

These transformations act as similarity transformations on the points. Do they change the image of the absolute conic and the line image plane so as to correctly reflect the transformation

induced on the points? In other words, say c_x , c_y , and f are fixed, applying T_τ would induce a translation of τ on points; it should therefore transform $\tilde{\omega}$ into

$$(c_x + \tau_x, c_y + \tau_y, (c_x + \tau_x)^2 + (c_y + \tau_y)^2 + 4f^2 - \frac{1}{4}, 1)^T,$$

and the line image plane (11) to

$$2p(c_x + \tau_x) + 2q(c_y + \tau_y) - r = (c_x + \tau_x)^2 + (c_y + \tau_y)^2 + \frac{1}{4},$$

so that the new image center is $(c_x + \tau_x, c_y + \tau_y)$ as desired; any rotation or scaling should act similarly. One can verify that all four transformations transform $\tilde{\omega}$ and the line image plane in a manner consistent with the way in which the transformations affect points.

Thus, there is a linear transformation taking point representations of image points obtained from a camera with intrinsic parameters c_x , c_y , and f , to calibrated rays. This transformation is the 4×4 matrix,

$$K = S_{\frac{1}{4f}} T_{(-c_x, -c_y)} \quad (12)$$

$$= \begin{pmatrix} 4f & 0 & 0 & -4c_x f \\ 0 & 4f & 0 & -4c_y f \\ -2c_x & -2c_y & 1 & \frac{1}{4} + c_x^2 + c_y^2 - 4f^2 \\ 0 & 0 & 0 & 16f^2 \end{pmatrix}. \quad (13)$$

This is an important point, for if $q = (u, v, 1)^T$ is the parabolic projection (with intrinsics c_x , c_y , f) of the space point $p = (x, y, z, 1)^T$ then for some scalar λ ,

$$p = \lambda K \left(u, v, u^2 + v^2 - \frac{1}{4}, 1 \right)^T.$$

Implying that if

$$P = \begin{pmatrix} 1 & 0 & 0 & 0 \\ 0 & 1 & 0 & 0 \\ 0 & 0 & 1 & 0 \end{pmatrix},$$

then

$$PK \left(u, v, u^2 + v^2 - \frac{1}{4}, 1 \right)^T \propto \left(\frac{x}{z}, \frac{y}{z}, 1 \right) \quad (14)$$

which is the **perspective projection** of $(x, y, z, 1)$ with image center $(0, 0, 1)$ and focal length $f = 1$. Note that K is different from the usual camera matrix: it is not actually a projection; P induces the projection. Leaving K non-singular (i.e. not incorporating P) will make it easier to prove that a matrix, a fundamental matrix, created with it has a certain rank.

2.4 The Catadioptric Fundamental Matrix

Let m and n be calibrated rays pointing to the same point $(x, y, z, 1)$ in space taken from two views related by a rotation R and translation t . The points m and n must satisfy the epipolar constraint which is specified by

$$n^T [t]_\times R m = n^T E m = 0, \quad (15)$$

where $E = [t]_{\times} R$ is called the essential matrix. Say $p = (u_1, v_1, 1)^T$ and $q = (u_2, v_2, 1)^T$ are two parabolic catadioptric projections of the space point, and say the camera matrices are K and K' , with $\tilde{\omega}$ and $\tilde{\omega}'$ the point representations of the image of the absolute conic. If \tilde{p} and \tilde{q} are their liftings to Π , then using equation (14), so that $m = PK\tilde{p}$ and $n = PK'\tilde{q}$, the epipolar constraint (15) becomes,

$$\tilde{q}^T K'^T P^T EPK\tilde{p} = 0. \quad (16)$$

Let the 4×4 matrix

$$F = K'^T P^T EPK \quad (17)$$

be called the *catadioptric fundamental matrix*. Then the epipolar constraint for parabolic catadioptric cameras is

$$\tilde{q}^T F\tilde{p} = 0. \quad (18)$$

Theorem. *The catadioptric fundamental matrix defined in (17) has rank 2. Let $\tilde{\omega}_1$ be the point representation of the image of the absolute conic in the first image, corresponding to K , and similarly for $\tilde{\omega}_2$ corresponding to K' in the second image. Then,*

$$\tilde{\omega}_2 F = 0 \quad \text{and} \quad F\tilde{\omega}_1 = 0. \quad (19)$$

Proof: The essential matrix E is known to be of rank 2, thus $P^T EP = \begin{pmatrix} E & 0 \\ 0 & 0 \end{pmatrix}$ has rank 2. Since K and K' are non-singular then F must also have rank 2. Let us calculate the left and right null vectors of F . First, let t and t' be the images of the viewpoints from each camera,

$$t'^T E = 0, \quad \text{and} \quad Et = 0.$$

Then by inspection, linearly independent left and right null vectors of $P^T EP$ are

$$f_1 = \begin{pmatrix} t'^T & 0 \end{pmatrix}, \quad f_2 = \begin{pmatrix} 0 & 0 & 0 & 1 \end{pmatrix} \quad \text{and}$$

$$f'_1 = \begin{pmatrix} t & 0 \end{pmatrix}^T, \quad f'_2 = \begin{pmatrix} 0 & 0 & 0 & 1 \end{pmatrix}^T.$$

Hence $g_{i=1,2} = K^{-1}f_i$ are vectors spanning the right nullspace of F and $g'_{i=1,2} = f'^T_i K'^{-T}$ are vectors spanning the left nullspace. Note that $g_2 = \tilde{\omega}_1$ and $g'_2 = \tilde{\omega}_2^T$. Therefore,

$$\tilde{\omega}_2^T F = 0 \quad \text{and} \quad F\tilde{\omega}_1 = 0.$$

Corollary. *If $K = K'$ and $t \neq t'$ then,*

$$\ker F \cap \ker F^T = \{\lambda \tilde{\omega}\}.$$

The condition $t \neq t'$ is true when the rotation is not trivial and when the axis of rotation is not the translation vector.

3 Algorithm

The algorithm proceeds in three steps. First estimate the fundamental matrix, from the fundamental matrix extract the intrinsic parameters via the image of the absolute conic, and reconstruct using well known perspective methods.

Estimating F

We use a non-linear method to estimate F . An algorithm based on singular value decomposition which is similar to the the 8-point algorithm for the perspective case exists for parabolic catadioptric projections but is equally sensitive.

1. Obtain images $p_{i,j} = (u_{i,j}, v_{i,j}, 1)^T$ of the same point $q_{j=1,\dots,n}$ in space in two catadioptric views $i = 1, 2$. Let

$$\tilde{p}_{i,j} = \left(u_{i,j}, v_{i,j}, u_{i,j}^2 + v_{i,j}^2 - \frac{1}{4}, 1 \right)^T.$$

2. Minimize the sum of first-order geometric errors,

$$\sum_j \frac{(\tilde{p}_{2,j} F \tilde{p}_{1,j})^2}{(F \tilde{p}_{2,j}) \circ (F \tilde{p}_{2,j}) + (F^T \tilde{p}_{1,j}) \circ (F^T \tilde{p}_{1,j})},$$

where the minimization is over F and using the notation $p \circ q = p \begin{pmatrix} 1 & 0 & 0 & 0 \\ 0 & 1 & 0 & 0 \\ 0 & 0 & 1 & 0 \\ 0 & 0 & 0 & 0 \end{pmatrix} q$. F is

parameterized as in:

$$\begin{pmatrix} a & b & \alpha a + \beta b & \gamma a + \delta b \\ c & d & \alpha c + \beta d & \gamma c + \delta d \\ e & f & \alpha e + \beta f & \gamma e + \delta f \\ g & h & \alpha g + \beta h & \gamma g + \delta h \end{pmatrix},$$

where one of a, \dots, f is held constant at 1. This ensures that F has rank 2. Initial estimates for F can be obtained using the singular value decomposition method since the components of F are linear in coordinates of the lifted image points.

Estimating ω

In the case where $K = K'$ the left and right nullspaces of F contain the point representation of the image of the absolute conic. In the presence of noise the nullspaces will not intersect. Once we have calculated the two-dimensional nullspaces, we choose the point equidistant to the two lines as the estimate of $\tilde{\omega}$.

When the intrinsics vary and we have images from three views, with three matrices $K_{i=1,2,3}$ and point representations $\tilde{\omega}_{i=1,2,3}$, we then have

$$\begin{aligned} F_{12} &= K_2^T P^T E_{12} P K_1, \\ F_{23} &= K_3^T P^T E_{23} P K_2, \\ F_{31} &= K_1^T P^T E_{31} P K_3. \end{aligned}$$

Then once we have estimated the three fundamental matrices we calculate say $\tilde{\omega}_1$ from the fact that,

$$\ker F_{12} \cap \ker F_{31}^T = \{\tilde{\omega}_1\}.$$



Figure 5: Two images taken with the same parabolic catadioptric camera. Points are those used for correspondence. Points highlighted in white are on the ground plane; points highlighted in black are on one side of the building facade.

Again, the estimate of $\tilde{\omega}_1$ is the point equidistant to the two nullspaces.

Reconstruction

Reconstruction proceeds as in the calibrated perspective case. Once we have determined $\tilde{\omega}$ and consequently ω , we can transform the image points into calibrated rays with which we determine the essential matrix E using a non-linear optimization and then back-project the rays into space using a linear algorithm, both algorithms described in (Hartley & Zisserman, 2000).

4 Experiments

We use the algorithm to perform a reconstruction of a scene from two views. The two pictures in Figure 5 are of a building on the campus of our institution and are assumed to have the same intrinsic parameters. First we manually choose and correspond points in the two images. We calculate the fundamental matrix F between the two views from the point correspondences using the algorithm described in the previous section. We estimate the point representation of the image of the absolute conic by finding the left and right nullspaces of F and finding the point equidistant to each. Using the intrinsic parameters we back-project the image points to calibrated rays. Using the calibrated rays we estimate the essential matrix E , decompose E into translation and rotation, and determine the perspective camera projection matrices P_1 and P_2 . We then back-project the rays and use homogeneous linear triangulation to estimate scene points.

The reconstruction is shown in the top and bottom of Figure 6. In the reconstruction we have fitted a plane to the points on the front facade of the building and to points on the ground plane, these are highlighted in Figure 5 and shaded differently in Figure 6. The viewpoints and poses are also displayed in the figures. The triangulation is manually added and shown for visualization purposes only. The ground plane and front facade were reconstructed to almost planar surfaces and are close to perpendicular. The other facade of the building, on the left in the images, did not reconstruct true to the scene, this is because this plane is perpendicular to the axis of motion which makes estimating depth more error-prone. In two views with such small motion, the

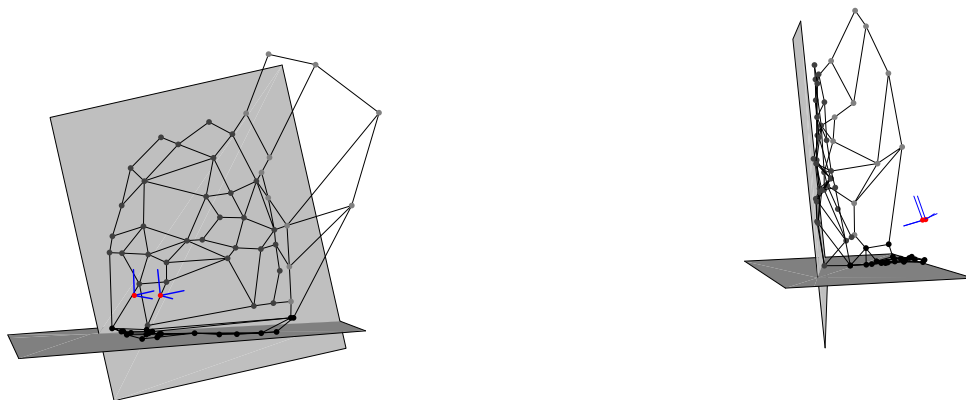


Figure 6: Reconstruction from two images. Black points are in the ground plane. Darkly shaded points are on the front facade of the building; lightly shaded points are on the other facade (which is on the left in the images). Planes are fitted to the facade and ground plane (and translated slightly so points are made visible). The coordinate systems at the points are the pose estimates. Tilt of the fitted plane is irrelevant to the results of the reconstruction. The top view is taken looking straight at the front facade; the bottom view is from the side. Note that the mirror reverses the orientation; this has been accounted for in the reconstruction.

reconstruction performs remarkably well.

5 Conclusion

We have established a new representation for images of lines and points in parabolic catadioptric video. Based on this representation we found a natural representation for the image of the absolute conic if aspect ratio and skew are assumed known. Writing the epipolar constraint in this new space yields a new catadioptric fundamental matrix. It turns out that the image of the absolute conic belongs to the two-dimensional kernel of this matrix. Applying thus only subspace recovery and intersection we can obtain Euclidean reconstructions:

- from two views with the same camera
- from three views with three different cameras.

The corresponding minimal views for the perspective case are three and four, respectively. This approach opened new questions some of which we address in our current work (Geyer & Daniilidis, 2002b): What is the number of independent conditions on F to be decomposable? What is the degree of the manifold of all catadioptric fundamental matrices? Which point configurations make the recovery of the fundamental matrix degenerate?

Sensor resolution of commercial catadioptric cameras is increasing every year. We believe that geometrically intuitive algorithms working directly on catadioptric images can provide flexible solutions for novel view synthesis from omnidirectional video as well as for fast and robust localization.

References

- Aliaga, D., & Carlbom, I. (2001). Plenoptic Stitching: A Scalable Method for Reconstructing Interactive Walkthroughs. In *Proceedings of ACM SIGGRAPH*, pp. 443–450.
- Antone, M., & Teller, S. (2000). Automatic Recovery of Relative Camera Rotations in Urban Scenes. In *IEEE Conf. Computer Vision and Pattern Recognition* Hilton Head Island, SC, June 13-15.
- Barreto, J., & Araujo, H. (2002). Issues on the Geometry of Central Catadioptric Imaging. In *Hawaii, Dec. 11-13*, Vol. IV, pp. 422–427.
- Benosman, R., & Kang, S. (2000). *Panoramic Vision*. Springer-Verlag.
- Benosman, R., & Mouaddib, E. (Eds.). (2002). *Workshop on Omnidirectional Vision*, Copenhagen, June 2. IEEE Computer Society Press.
- Boult, T. (1998). Remote reality demonstration. In *IEEE Conf. Computer Vision and Pattern Recognition*, pp. 966–967 Santa Barbara, CA, June 23-25.
- Bruckstein, A., & Richardson, T. (2000). Omniview cameras with curved surface mirrors. In *IEEE Workshop on Omnidirectional Vision, Hilton Head, SC, June 12*, pp. 79–86. originally published as Bell Labs Technical Memo, 1996.
- Chen, E., & Williams, L. (1993). View Interpolation for Image Synthesis. In *Proceedings of ACM SIGGRAPH*.
- Daniilidis, K. (Ed.). (2000). *IEEE Workshop on Omnidirectional Vision*, Hilton Head Island, SC, June 12.
- Daniilidis, K., Makadia, A., & Bülow, T. (2002). Image Processing in Catadioptric Planes: Spatiotemporal Derivatives and Optical Flow Computation. In *Workshop on Omnidirectional Vision, Copenhagen, June 22*, pp. 3–12.
- Daniilidis, K., & Spetsakis, M. (1996). Understanding noise sensitivity in structure from motion. In Aloimonos, Y. (Ed.), *Visual Navigation*, pp. 61–88. Lawrence Erlbaum Associates, Hillsdale, NJ.
- Faugeras, O., Luong, Q.-T., & Papadopoulos, T. (2001). *The Geometry of Multiple Images: The Laws That Govern the Formation of Multiple Images of a Scene and Some of Their Applications*. MIT Press.
- Fermüller, C., & Aloimonos, Y. (1998). Ambiguity in structure from motion: Sphere vs. pla. *International Journal of Computer Vision*, 28, 137–154.
- Geyer, C., & Daniilidis, K. (2001a). Catadioptric projective geometry. *International Journal of Computer Vision*, 43, 223–243.
- Geyer, C., & Daniilidis, K. (2001b). Structure and motion from uncalibrated catadioptric views. In *IEEE Conf. Computer Vision and Pattern Recognition* Hawaii, Dec. 11-13.
- Geyer, C., & Daniilidis, K. (2002a). Para-cata-dioptic calibration. *IEEE Trans. Pattern Analysis and Machine Intelligence*, 24, 687–695.

- Geyer, C., & Daniilidis, K. (2002b). Properties of the Catadioptric Fundamental Matrix. In *Proc. Seventh European Conference on Computer Vision*, pp. 140–154 Copenhagen, Denmark.
- Gluckman, J., & Nayar, S. (1998). Ego-motion and omnidirectional cameras. In *Proc. Int. Conf. on Computer Vision*, pp. 999–1005 Bombay, India, Jan. 3-5.
- Gortler, S., Grzeszczuk, R., Szeliski, R., & Cohen, M. (1996). The lumigraph. In *Proceedings of ACM SIGGRAPH*, pp. 43–54.
- Hartley, R., & Zisserman, A. (2000). *Multiple View Geometry*. Cambridge Univ. Press.
- Heyden, A., & Aström, K. (1997). Euclidean reconstruction from image sequences with varying and unknown focal length and principal point. In *IEEE Conf. Computer Vision and Pattern Recognition*, pp. 438–443.
- Jepson, A., & Heeger, D. (1990). Subspace methods for recovering rigid motion II: Theory. Tech. rep. RBCV-TR-90-36, University of Toronto.
- Kang, S. (2000). Catadioptric self-calibration. In *IEEE Conf. Computer Vision and Pattern Recognition*, pp. I-201–207 Hilton Head Island, SC, June 13-15.
- Levoy, M., & Hanrahan, P. (1996). Lightfield Rendering. In *Proceedings of ACM SIGGRAPH*, pp. 31–42.
- Ma, Y., Soatto, S., Kosecka, J., & Sastry, S. (2000). Euclidean Reconstruction and Reprojection up to Subgroups. *International Journal of Computer Vision*, 38, 217–227.
- Maybank, S. (1993). *Theory of Reconstruction from Image Motion*. Springer-Verlag, Berlin et al.
- Maybank, S., & Faugeras, O. (1992). A theory of self-calibration of a moving camera. *International Journal of Computer Vision*, 8, 123–151.
- Mulligan, J., Isler, V., & Daniilidis, K. (2002). Trinocular Stereo: A New Algorithm and its Evaluation. *International Journal of Computer Vision*, 47, 51–61.
- Nayar, S. (1997). Catadioptric Omnidirectional Camera. In *IEEE Conf. Computer Vision and Pattern Recognition*, pp. 482–488 Puerto Rico, June 17-19.
- Pedoe, D. (1970). *Geometry: A comprehensive course*. Dover Publications, New York, NY.
- Pollyfeys, M., Koch, R., & van Gool, L. (1998). Self-calibration and Metric Reconstruction in Spite of Varying and Unknown Internal Camera Parameters. In *Proc. Int. Conf. on Computer Vision*, pp. 90–95 Bombay, India, Jan. 3-5.
- Rees, D. W. (1971). Panoramic television viewing system. United States Patent No. 3, 505, 465, Apr. 1970.
- Sturm, P. (1999). Critical Motion Sequences for the Self-Calibration of Cameras and Stereo Systems with Variable Focal Length.. In *BMVC*.
- Sturm, P. (2002). Mixing Catadioptric and Perspective Cameras. In *Workshop on Omnidirectional Vision, Copenhagen, June 22*, pp. 37–44.

- Svoboda, T., Pajdla, T., & Hlavac, V. (1998). Epipolar geometry for panoramic cameras. In *Proc. 5th European Conference on Computer Vision*, pp. 218–231.
- Taylor, C. (2000). Video Plus. In *IEEE Workshop on Omnidirectional Vision, Hilton Head, SC, June 12*, pp. 3–10.
- Yagi, Y., Kawato, S., & Tsuji, S. (1994). Real-time omnidirectional image sensor (COPIS) for vision-guided navigation. *IEEE Trans. on Robotics and Automation*, 10, 11–22.